JOURNAL OF VIROLOGY, Mar. 1995, p. 1408–1419 Vol. 69, No. 3
0022-538X/95/$04.00+0

Induction of Focal Spongiform Neurodegeneration in Developmentally Resistant Mice by Implantation of Murine Retrovirus-Infected Microglia

WILLIAM P. LYNCH,* SHELLY J. ROBERTSON, AND JOHN L. PORTIS

Laboratory of Persistent Viral Diseases, Rocky Mountain Laboratories, National Institute of Allergy and Infections Diseases, Hamilton, Montana 59840

Received 12 July 1994/Accepted 14 November 1994

FrCas^E is a highly neurovirulent murine leukemia virus which causes a noninflammatory spongiform neurodegenerative disease after neonatal inoculation. The central nervous system (CNS) infection is widespread, involving several different cell types, whereas the lesions are localized to motor areas of the brain and spinal cord. Inoculation of FrCas^E at 10 days of age (P10) results in viremia, but infection of the CNS is restricted and neurological disease is not observed (M. Czub, S. Czub, F. McAtee, and J. Portis, J. Virol. 65:2539–2544, 1991). In this study, we used this developmental resistance to restrict the extent and the distribution of FrCas^E in the brain to examine whether the spongiform degeneration is a consequence of infection of cells in proximity to the lesions. Two approaches were used to infect the brain on or after P10. First, mice were inoculated with FrCas^E at P10 to induce viremia and then at P17 were subjected to focal CNS injury within brain regions known to be susceptible to virus-induced spongiform degeneration. The injury resulted in local inflammation, glial activation, migration of inflammatory cells into the wound site, and high-level parenchymal infection about the wound site. However, no evidence of spongiform neurodegeneration was observed over a period of 3 months. The second approach involved the implantation of FrCas^E-infected microglia into the CNS at ≥P10. This resulted in microglial engraftment and focal CNS infection unilaterally at the implantation sites and bilaterally along white matter tracts of the corpus callosum and pons and in cells of the subventricular layers of the lateral cerebral ventricles. Strikingly, focal spongiform degeneration colocalized with the sites of infection. In contrast to the wounding experiments, the implantation model was not associated with an inflammatory response or significant glial activation. Results of these studies suggest that (i) the developmental resistance of the CNS to infection lies at the blood-brain barrier and can be bypassed by direct introduction into the brain of virus-infected cells, (ii) the neuropathology induced by this virus is a consequence of local effects of the infection and does not appear to require endothelial or neuronal infection, and (iii) elements of the inflammatory response and/or glial activation may modulate the expression of neuropathology induced by neurovirulent retroviruses.

FrCas^E is a chimeric murine leukemia virus which contains the envelope gene and 3′ *pol* sequences of the wild mouse ecotropic retrovirus CasBrE in a Friend murine leukemia virus background (56). It causes a rapid noninflammatory spongiform neurodegenerative disease involving primarily the motor centers of the brain and spinal cord (14, 46, 56). After neonatal intraperitoneal inoculation at 1 day of age (P1), FrCas^E replicates rapidly in the periphery and enters the brain by P6, at which time endothelial cells and pericytes are infected. This is followed by the infection of microglial cells and certain populations of neurons which undergo cell division postnatally (14). The infected neurons, which include cells of the cerebellar cortex, hippocampus, and olfactory bulb, exhibit no evidence of cytopathology at either the light or electron microscopic level (46). Furthermore, the neurons which exhibit pathologic changes express neither virus-specific mRNA nor viral protein (46). It has therefore been argued that this disease is an indirect consequence of virus infection.

We observed that infected microglial cells appear to be concentrated in sites exhibiting spongiform degeneration, suggesting their possible importance in disease pathogenesis (46). This observation has also been made for two other neurovirulent murine retroviruses, Moloney *ts*1 (4, 5) and CasBrE (30). In addition, we reported that microglial cells grown in vitro exhibit a defect in posttranslational processing of the envelope precursor polyprotein pr85^{env} (45), a property which has been suggested to be important in some forms of retrovirus-induced neurodegeneration (reviewed in reference 66). Direct proof of the importance of microglial cells has not been forthcoming, and one cannot formally exclude participation of other cell types either proximal to the spongiform degeneration (e.g., endothelial cells) or, perhaps, remote to the affected motor centers. The latter possibility has been raised because cerebellar cortical neurons are heavily infected by both CasBrE (30, 37) and FrCas^E (46), and these cells indirectly make downstream synaptic contacts with virtually the entire motor system.

In contrast to neonatally inoculated mice, when FrCas^E is inoculated into mice at P10, the virus replicates in the periphery but the mice do not develop neurological disease. This age-dependent resistance is a consequence of an intrinsic central nervous system (CNS)-specific restriction of virus infection which develops as a function of as yet unknown, postnatal developmental factors (12, 13). In these mice, there is neither immunohistochemical evidence of virus expression in the CNS nor any evidence of spongiform degeneration (12, 44). In the current study, we have used this age-dependent resistance to restrict the otherwise widespread distribution of FrCas^E in the

* Corresponding author. Present address: Department of Pathology, Brigham and Women's Hospital, Harvard Medical School, LMRC 514, 221 Longwood Ave., Boston, MA 02115. Phone: (617) 278-0316. Fax: (617) 732-5795.

CNS. Two approaches were used in an attempt to achieve focal infection of parenchymal cells in the CNS. The first involved the induction of a wound response in mice in which a viremia was produced by inoculation of $FrCas^E$ at P10. The second approach was to introduce $FrCas^E$-infected microglial cells into the brains of developmentally resistant mice under conditions in which minimal CNS inflammation was observed. The brain wounding of viremic mice resulted in local inflammation, glial activation, and a significant localized CNS infection. However, this infection was not associated with spongiform degeneration. In contrast, the transplantation of infected microglia into the brain resulted in significant focal CNS infection both ipsi- and contralateral to the injection sites, accompanied by the colocalization of focal spongiform degeneration. These studies indicate that the developmental restriction to virus infection could be bypassed by breaching the blood-brain barrier and that the induction of neuropathology appeared to be due to local effects of virus infection. Data from the wound experiment further suggest that factors associated with the inflammatory response and/or glia activation may modulate the expression of the retrovirus-induced spongiform degeneration.

MATERIALS AND METHODS

Virus, cells, and mice. All the mice used in these studies were IRW (Inbred Rocky Mountain White) mice bred and raised at Rocky Mountain Laboratories. These mice are highly susceptible to the neurodegenerative disease caused by the CasBrE virus and the $FrCas^E$ chimeric retrovirus derived from it (56). The chimeric $FrCas^E$ virus was prepared from Fischer rat embryo cells as described previously (56). Virus stocks contained 2.1×10^6 to 2.3×10^6 focus-forming units (FFU)/ml. Mouse viremia titers were determined by the focal immunoassay previously described (12).

Microglia were prepared from neonatal IRW mice as described by Lynch et al. (45). Briefly, mixed glial cultures were made as described previously (41) and grown on poly-D-lysine-coated flasks. When the cultures reached 50% confluence, they were infected with $FrCas^E$ virus at a multiplicity of infection of 1 for 1 h in the presence of 8 μg of Polybrene per ml. Medium was changed every other day, and the cultures were grown until many phase-bright cells could be identified growing over a confluent monolayer. Enriched microglial fractions were obtained by shaking (180 rpm) the mixed glial cultures for 4 h at 37°C. Plating and immunostaining of the shake-off-released cells for microglial antigens F4/80 (2) and Mac-1 (62) indicated that more than 98% of this fraction were microglial cells, consistent with our earlier report (45). Immunostaining of the shake-off population by using virus-specific anti-gp70 monoclonal antibody 667 (49) indicated that more than 95% of these cells were positive for infection (45). The released microglial cells were concentrated by centrifugation for 5 min at $700 \times g$, washed two times with RPMI 1640 medium supplemented with 2% fetal calf serum (HyClone), and resuspended at approximately 10^7 cells per ml prior to injection into the brains of IRW mice.

Virus inoculation and brain wounding. For the brain wounding experiments, one group of IRW mice (48 pups) was inoculated intraperitoneally with 100 μl of $FrCas^E$ virus stock at P10, while a second group (32 pups) was not inoculated. At P17, 30 mice from the inoculated group and 19 mice from the uninoculated group were deeply anesthetized by Metofane inhalation and brain wounded by using a flame-heated 25-gauge needle as outlined below. A midline incision was made over the skull, and the skin was retracted. The needle was then inserted through the skull over the left hemisphere of the cortex down to the thalamus for approximately 20 s. The needle was inserted by hand approximately 6 mm deep at a position corresponding to approximately 2 mm lateral and 5 mm rostral of the intersection of the transverse and longitudinal cerebral fissures. After removal of the needle, the skin was closed with small wound clips. Animals were kept warm until they recovered from the anesthesia and were then returned to their mothers. No mortality or clinical neurologic signs were observed for any of the animals used through the course of these experiments. Animals were killed under Metofane inhalation anesthesia at 7, 14, 30, 60, or 90 days postwounding to assay for viremia, CNS infection, and CNS histopathology. All 10-day-old $FrCas^E$-inoculated animals had circulating viremia of 10^3 FFU/ml or greater at the time of killing.

CNS implantation of microglial cells. For the CNS implantation experiments, P10 IRW mice were anesthetized under Metofane, a 1-cm midline incision was made in the scalp, and the skin was retracted. $FrCas^E$-infected microglia, uninfected microglia, $FrCas^E$ virus, or medium alone was injected by using a glass micropipette (made as described previously [32]) to minimize trauma. Injections were made at up to three sites in the left cortical hemispheres down into the thalamus and one site in the colliculus (indicated in Fig. 1). Injections were begun once the micropipette was fully inserted (approximately 4 mm) and continued until the pipette tip was removed from the skull. This resulted in an injection of 1 to 3 μl (total volume) at each site (approximately 2×10^4 microglial cells or 5×10^3 FFU of free virus). The injection volume was kept small to minimize the loss of cells and virus from the CNS. Infectious units injected into the CNS of the mice receiving virus or cells were reasonably comparable, since we had previously found in vitro that 2×10^4 microglial cells generate approximately 1 FFU/24 h but score as infectious centers at approximately 50% efficiency (45).

The scalp was closed with wound clips, and the mice were kept warm until they recovered from the anesthesia. P10 IRW mice were very susceptible to overdoses of Metofane regardless of whether surgical procedures were performed, and thus careful monitoring was necessary to ensure a high survival rate. For the experiments reported herein, survival was over 95%. All experimental mouse pups were allowed to nurse on their mothers until they were 3 weeks old, at which time they were weaned and sexed. Animals did not show any clinical manifestation of neurological disease throughout the course of these experiments. Animals were killed at 5, 7, 10, 12, and 21 days postimplantation for evaluation of viremia and spleen and CNS infection and at 12 and 21 days for CNS histopathology. A minimum of four animals were evaluated per time point per experimental group.

To monitor the fate of the injected cells, some mice were injected with microglial cells (infected and uninfected) which had phagocytosed acetylated low-density lipoprotein labeled with the fluorescent dye 1,1′-dioctodecyl-3,3,3′,3′-tetramethyl indocarbocyaninate (DiI-AcLDL; Molecular Probes) as previously described (45) or by using the cell surface label PHK-26 as instructed by the manufacturer (Sigma) (33). Mice receiving labeled cells were killed at 5, 12, and 21 days postimplantation. Again, a minimum of four animals per time point were evaluated. Cells were detected in 20-μm frozen sections, which were fixed in 10% formalin and viewed in a Leitz epifluorescence microscope equipped with a rhodamine filter set.

Histopathology and immunohistochemistry. Pathologic changes were examined in the brains of all mice by using standard histological techniques. Mice were anesthetized and perfused through the left ventricle for 10 min, using 10% formalin in 50 mM phosphate buffer (pH 7.0). Brains were removed and fixed for an additional 4 h at room temperature, dehydrated, and embedded in paraffin. Brain sections of 4 μm were taken at approximately 100-μm intervals beginning just caudal to the olfactory bulbs and proceeding through the medulla. Sections were stained with hematoxylin and eosin and viewed by bright-field microscopy.

Immunohistochemistry was performed as previously described, using fresh frozen or paraformaldehyde-lysine-periodate (PLP)-fixed tissue (46, 47). Viral gp70-specific monoclonal antibodies biotinylated 667 (667B) (46, 49) and 83A25 (17) were used to detect sites of virus infection. Detection of microglia and monocyte/macrophage cell types was accomplished by using monoclonal antibodies Mac-1 (62) and F4/80 (2). Biotinylated ricin communis agglutinin 1 (RCA-1; Vector) was also used on sections from normal control mice and those transplanted with microglia; however, significant reactivity was not noted. Endothelial cells were detected by using rabbit anti-factor VIII (Biogenex). Oligodendroglia were detected by using rabbit antigalactocerebroside (Chemicon), rabbit anti-glycerol-3-phosphate dehydrogenase (Chemicon), rabbit anti-myelin basic protein (Biogenex), and sheep anti-carbonic anhydrase II (Biodesign) on frozen sections. Astrocytes were detected by using rabbit anti-S-100 protein (Biogenex) in frozen sections or anti-cow glial fibrillary acidic protein (GFAP; Dako) in paraffin sections after xylene extraction and rehydration or in PLP-fixed tissue sections after a 5-min wash in 0.1% Triton X-100 in phosphate-buffered saline. A variety of rat monoclonal antibodies were used to identify infiltrating leukocytes in the stab-wounded animals: RM2.2, anti-CD2 (67); KT3-1.1, anti-CD3 (64); 191.1.2, anti-CD4 (9); 53-7.313, anti-CD5 (39); 169-4, anti-CD8 (9); B220, RA3-6B2, anti-CD45 B-cell isomer (10); Gr1, RB6-8C5, anti-neutrophil (31); and biotinylated GK1.5, anti-CD4 (15). The rat anti-blood cell antibodies were generously provided by G. Spangrude at Rocky Mountain Laboratories. Primary antibodies were detected by using species-specific biotinylated secondary antibodies (Vector) followed by Supersensitive peroxidase-coupled streptavidin (Biogenex); when the primary reagent was biotinylated, detection required only the use of Supersensitive peroxidase-coupled streptavidin. Alternatively, biotinylated reagents were detected by using fluorescein isothiocyanate coupled to avidin-D (Vector) in experiments colocalizing antigen and fluorescently tagged cells which had been transplanted. Aminoethyl carbazole was used as the peroxidase substrate, and the sections were counterstained with Mayer's hematoxylin. Sections were photographed directly, using Kodak Ektar 100 print film or Kodak Ektachrome 64 slide film. The latter was converted to prints by using an internegative.

RESULTS

CNS inflammation and viral infection in response to brain wounding. IRW mice, inoculated intraperitoneally with $FrCas^E$ at P10 to develop a peripheral viremia, were brain wounded through the left cerebral hemisphere into the thalamus at P17 (Fig. 1). These mice were evaluated immunohistochemically 7 days later for the presence of glial activation and viral infection

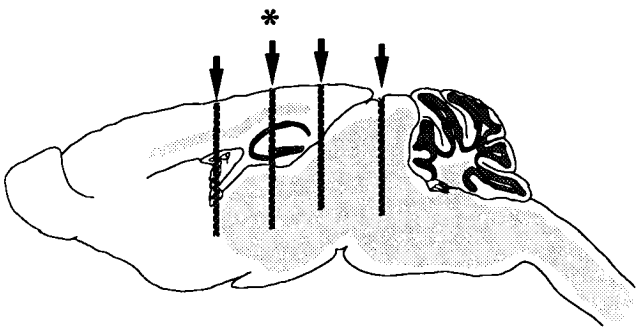

FIG. 1. Schematic diagram showing a sagittal view of the stab wound site (*) and virus or microglial injection sites in the mouse CNS (arrows and heavy bars). Shaded portions indicate areas which develop spongiform pathology after neonatal inoculation with $FrCas^E$ (14, 46).

in the CNS (P24). In response to the injury, astrocytes showed increased expression of GFAP (Fig. 2A) and microglial cells showed significant increases in Mac-1 and F4/80 monoclonal antibody staining (Fig. 2B and C, respectively). The wound site was also examined for the presence of additional leukocytes by using antibodies which recognized pan T- and B-cell markers as well as cytotoxic T cells, T-helper cells, granulocytes, thymocytes, and natural killer cells (see Materials and Methods). Occasionally, nonmonocytoid leukocytes were detected in the brains of the injured mice, but they were few in number and restricted to sites of acute damage along the needle track and were not apparent in the parenchyma (data not shown). These results are consistent with previously documented cellular changes occurring as a result of stab wounding (16, 25–27). Infected noninjured brains show very limited glial staining which was indistinguishable from that seen in uninfected noninjured controls (not shown).

Analysis of the region of the wound site for viral infection by using virus-specific anti-gp70 monoclonal antibodies (667B and 83A25 [46]) indicated that significant infection occurred along the entire length of the wound site which extended into the CNS parenchyma (Fig. 2D). This infection was readily detected in all mice examined at both 7 and 14 days postwounding ($n = 12$), indicating that the infection was not transient. The morphology of the infected cells in the parenchyma (Fig. 2F) was highly reminiscent of activated microglia, indicated by F4/80 immunostaining (Fig. 2E). The ramified nature indicates their origin from the brain rather than monocytes migrating in from the periphery. Evaluation of the contralateral side failed to show any detectable infection, suggesting that virus spread was limited to the vicinity of the stab site. No gp70-specific immunostaining was observed in uninfected brains which were stab wounded or in non-wounded brains from infected mice (not shown). The latter observation confirms the developmental resistance of the CNS to parenchymal infection (44).

Histological examination of wound-associated $FrCas^E$ infection. Given that we were able to consistently establish a local CNS infection in developmentally resistant mice, we examined whether this infection was inducing spongiform pathology. Histopathological analysis of the stab site of at least three mice per time point failed to reveal evidence of spongiform degeneration in the CNS parenchyma when examined 7, 14, 30, 60, and 90 days postwounding (Fig. 3E and F). No vacuolar pathology was noted even though the infection was present in regions (thalamus and cortex) which normally express pathology after neonatal infection by $FrCas^E$ (Fig. 3A and B). Examination of uninfected, CNS-wounded mice also showed no evidence of spongiform change at the wound site (Fig. 3C and D); and infected, nonwounded mice also did not express observable spongiform pathology (not shown) (12). The immunohistochemical and histopathological findings are summarized in Table 1. It is curious that no pathology was observable in the CNS despite the presence of significant virus infection, suggesting either that the presence of virus infection alone is not sufficient for pathology induction or that wounding may in some way prevent lesions from appearing.

Engraftment of $FrCas^E$-infected and uninfected microglia in the CNS of developmentally resistant mice. In a second approach, P10 mice were implanted intracerebrally with uninfected or $FrCas^E$-infected microglial cells at the sites diagrammed in Fig. 1. The inoculation time of P10 was chosen to limit the potential for significant glial activation (3, 48) while still taking advantage of the CNS resistance to infection. In addition, cells were introduced via a glass micropipette to further minimize the potential for trauma. In the present study, all mice inoculated with infected microglia at P10 developed viremia and splenic infection by the time they were killed; however, none of these mice expressed clinical neurological disease.

To determine whether $FrCas^E$-infected and uninfected microglia injected into the CNS would engraft, microglial cells were fluorescently labeled with either DiI-AcLDL (45) or PHK-26 (33) prior to implantation. Brains examined at 5, 12, and 21 days postimplantation showed the presence of fluorescently labeled cells at the implant sites (Fig. 4A and B) and more sparsely at distal sites along the corpus callosum, meninges, lateral ventricles, and choroid plexus (not shown). These sites are consistent with the normal locations of resident microglia/monocytoid cells in noninflamed brains (40, 58). No differences in engraftment were noted between cells labeled with the microglial cell-specific label DiI-AcLDL and the general cell label PHK-26, except that the latter label generally gave a stronger signal in vivo.

Immunohistochemical localization of $FrCas^E$ viral gp70 protein at 5, 12, and 21 days postimplantation indicated significant unilateral viral expression local to the injection sites (Fig. 4C and E) and bilateral expression of gp70 protein by cells in the corpus callosum (Fig. 4D and F) and subependymal germinal cells of the lateral ventricles (not shown). The periventricular and corpus callosal locations represent normal migratory pathways for developing microglia (40, 43, 58) as well as neurons and macroglia. High-magnification examination of the im-

FIG. 2. P17 stab wounding of developmentally resistant mice with a circulating viremia results in inflammation and local infection of the CNS parenchyma by 7 days postwounding (P24). Anti-GFAP staining (A) of a coronal section from the thalamus at the site of the stab wound (arrow) indicates an extensive astrocytic reaction. Staining for macrophage/microglial cells by using Mac-1 (anti-complement type 3 receptor) and F4/80 (B and C, respectively) indicates the presence of infiltrating monocytes in the stab site (arrows) and activation of parenchymal microglia (arrowheads). Staining for these microglial markers diminished quickly with increasing distance from the stab site. Immunoreactivity was undetectable on the contralateral side, consistent with staining observed in unwounded brains (not shown). Immunostaining for viral infection by using envelope-specific monoclonal antibody 667B shows extensive staining along the wound site (panel D, composite). In addition, many ramified cells adjacent to the wound itself express viral antigen (arrowheads). Higher-magnification comparison of F4/80-positive cells (E) and virally infected cells (F) in fresh-frozen sections indicates a similar ramified morphology (arrowheads), suggesting that the infected parenchymal cells were microglia. Similar results were obtained in mice 14 days postwounding. Magnifications: (A to D) ×46; (E and F) ×228.

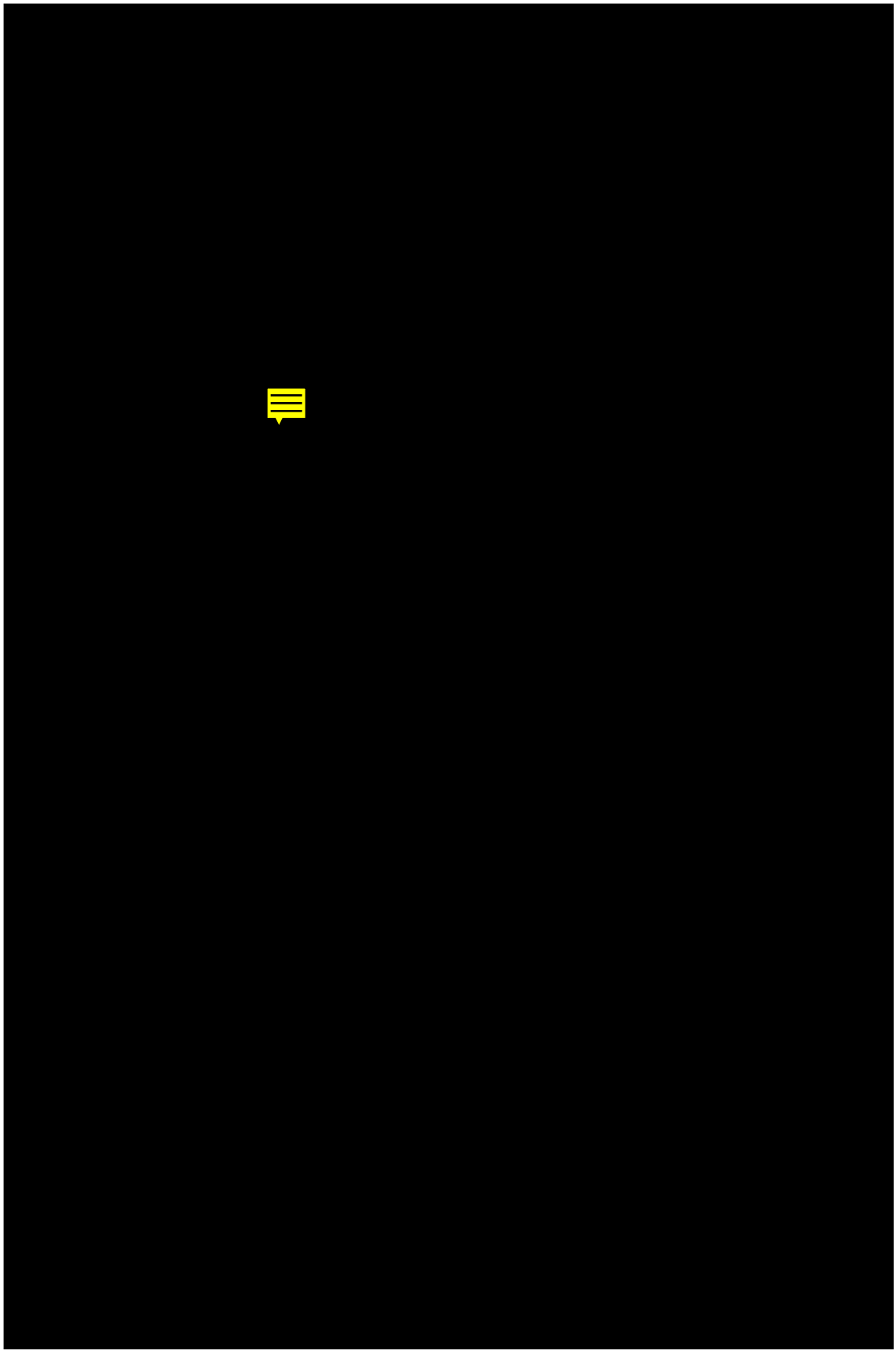

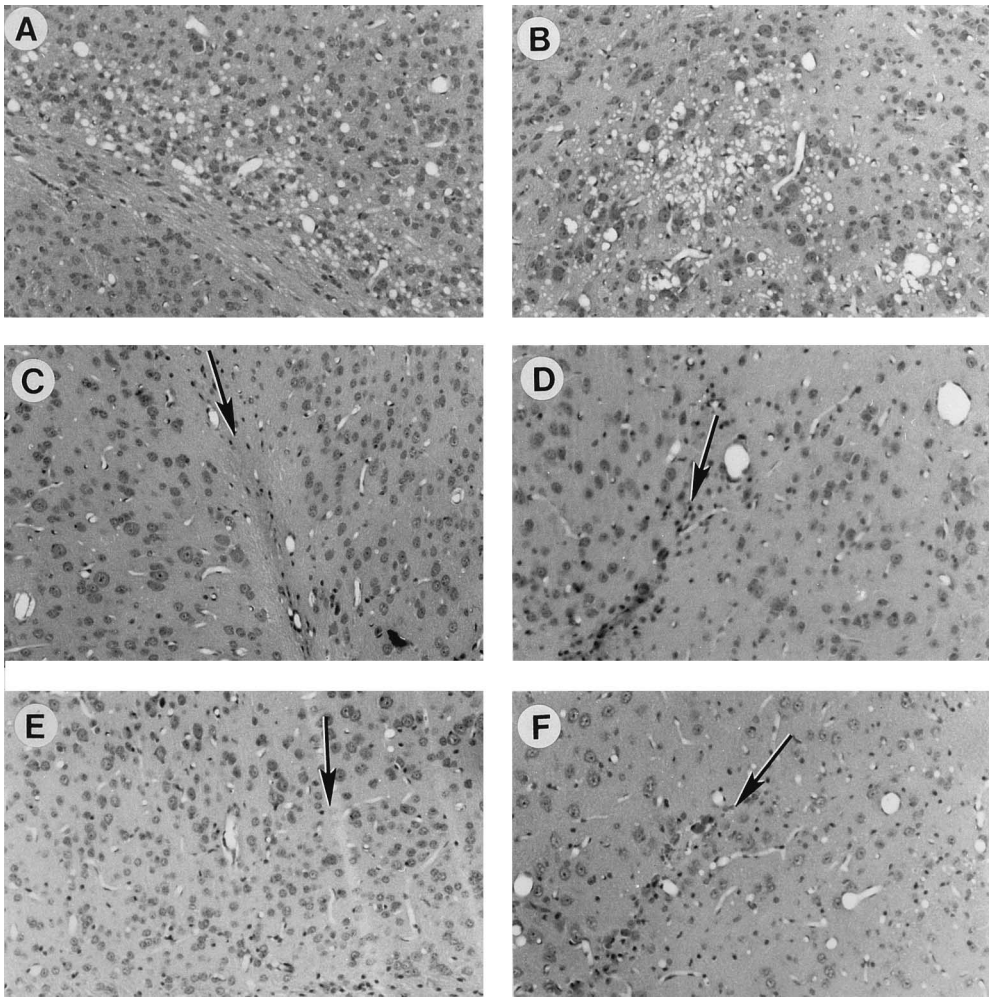

FIG. 3. Histological examination of the wound site fails to reveal evidence of virus-induced spongiform pathology. Shown are hematoxylin-and-eosin-stained coronal sections (4 μm) from the cerebral cortex (A, C, and E) and thalamus (B, D, and F) of IRW mice 16 days after neonatal inoculation with $FrCas^E$ (A and B), of P17 stab-wounded, uninfected mice 14 days postwounding (C and D), and of P17 stab-wounded, $FrCas^E$ infected mice 14 days postwounding (E and F). Note that the holes visible in panel F are associated with the microvasculature and do not represent spongiform neurodegeneration. Infected, wounded animals were also examined at 7, 21, 30, 60, and 90 days postwounding without observation of spongiform change (not shown). Arrows identify stab track. Magnifications, ×100.

plants (Fig. 4E and F) indicated the presence of infected cells possessing a highly ramified morphology. These cells were not limited to one site, indicating that spread of infection and cellular migration occurred after implantation.

The morphology of the infected cells suggested that they were primarily microglia; however, we were unable to identify them by using the markers Mac-1, F4/80, and RCA-1. This was surprising given that the microglia were strongly positive for these markers prior to implantation (45). This inability to detect both endogenous and transplanted microglia suggests that under these conditions, glial activation was minimal. The virus-positive cells also did not stain with antisera specific for astrocytes (anti-GFAP [7] or anti-S-100 protein [35]), oligodendroglia (antigalactocerebroside, anti-myelin basic protein, anti-carbonic anhydrase II, and anti-glycerol-3-phosphate dehydrogenase [63]), or endothelial cells (anti-factor VIII [35]), indicating that differentiated neuroglia and cells of the vasculature were not actively expressing virus (not shown). Although the majority of the infected cells resembled microglia, only a small proportion contained a fluorescent label. This finding suggests that endogenous CNS cells were infected in P10 mice.

TABLE 1. Summary of pathology and infection induced by different $FrCas^E$ virus challenges

Inoculation regimen[a]	Infection and pathology[b]					
	$FrCas^E$ infection			Spongiform pathology		
	Spleen	CNS	Clinical disease	White matter	Grey matter	Gliosis
PO–1 virus i.p. or i.c.	+++	+++	+++	+++	+++	−
P10 virus i.p.	+++	−	−	−	−	−
P10 i.p. + P17 wound	+++	++	−	−	−	+++
P17 wound only	−	−	−	−	−	+++
P10 i.c. no virus	−	−	−	−	−	+
P10 virus i.c.	+++	−[c]	−	±[c]	−	+
P10 normal Mg i.c.	−	−	−	−	−	+
P10 infected Mg i.c.	+++	++	−	++	++	+

[a] i.p., intraperitoneally; i.c., intracerebrally.

[b] −, not detected; ±, observed in a limited number of animals examined and present at very low levels; +, observed in all animals examined but at a very low level; ++, observed at high levels but highly localized; +++, observed at high levels and widespread.

[c] No virus infection of the CNS was detected in five animals even though a single focus of spongiform pathology was observed in two of five animals examined histopathologically.

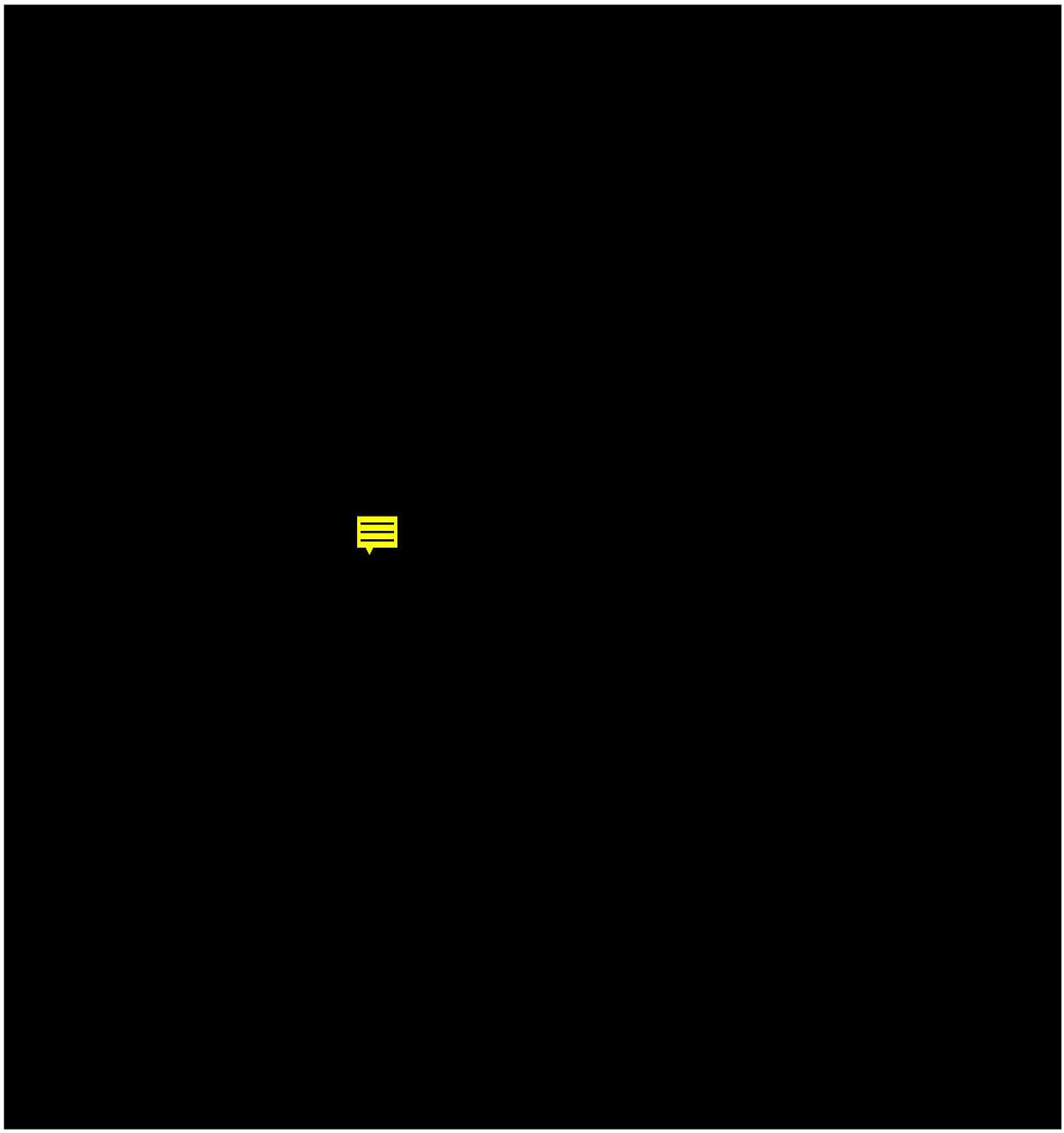

FIG. 4. Transplantation of microglial cells into P10 mice. Infected or uninfected microglial cells labeled with the aliphatic fluorescent chromophore PKH-26 (Sigma) and inoculated into P10 mice were detectable through the course of the experiment. (A) Labeled uninfected microglial cells (yellow-orange) in the cerebral cortex 10 days after inoculation. The corpus callosum is labeled in green, using rabbit antigalactocerebroside (Chemicon) followed by fluorescein isothiocyanate-labeled goat anti-rabbit immunoglobulin G. (B) Persistence of PKH-26 labeled $FrCas^E$-infected microglia in the thalamus 21 days after inoculation of a P10 mouse. Note the vesicular nature of the fluorescent cell marker in many of the labeled cells (arrowheads), indicating trafficking of the dye to an intracellular compartment. This latter phenomenon was also observed within 6 h of labeling in cells which were plated in vitro rather than transplanted (45). Immunohistochemical staining for viral envelope in horizontal sections of the mouse brain indicated unilateral viral expression local to the injection sites (C) and bilateral expression in cells of the subventricular germinal layer (not shown) and within the corpus callosum (D). Many of the virus-positive cells in the thalamus (E), colliculus (not shown), and corpus callosum (F) had highly ramified morphology (arrowheads) indicative of microglial cells. Magnifications: (A and B) ×180; (C and D) ×45; and (E and F) ×180. Micrographs for panels E and F were taken from 20-μm sections at a focal plane which could best represent the infected cell morphology at high magnification.

Another, less likely possibility is that the fluorescent marker might have been lost as a result of cell division of the labeled cells and thus marker dilution.

To further address the susceptibility of parenchymal cells to free exogenously added virus, IRW mice were microinjected with the $FrCas^E$ virus at P10. Expression of gp70 was not noted in animals examined at 10 ($n = 4$) and 21 ($n = 4$) days postinjection. This finding indicates that direct exposure to

virus was an inefficient means for infecting cells of the CNS and suggests the necessity for implantation of infected cells in order for significant viral infection to be observed. Interestingly, all animals inoculated with virus intracerebrally at P10 became viremic and had significant cellular infection in the spleen (not shown), indicating a high susceptibility to infection of cells in the periphery.

Pathology associated with microglial implantation. Histopathological examination of the brains of four mice at 12 days after implantation with $FrCas^E$-infected microglia failed to show evidence of spongiform degeneration; however, by 21 days postimplantation, all seven mice examined had spongiform lesions in areas in which infected cells were identified. Lesions appeared bilaterally in the deep layers of the motor cortex and the underlying corpus callosum (Fig. 5A and B) and at white-grey interfaces along the corticospinal tract in the pons (Fig. 5H). Unilateral spongiform lesions were observed in the thalamus (Fig. 5C), the colliculus (Fig. 5F), and the pons (Fig. 5G) at the sites of implantation. Analysis of other susceptible brainstem nuclei (e.g., the cochlear nucleus, the vestibular nucleus, and the spinal cord) which were distal to the sites of inoculation did not show any spongiform lesions, indicating that the effects of viral infection were local.

Brains which were inoculated with uninfected microglia or medium alone did not show any pathological changes. Animals intraperitoneally inoculated with the $FrCas^E$ virus at P10 also did not show evidence of spongiform pathology when examined 21 days postinoculation. Interestingly, examination of 5 animals in which $FrCas^E$ virus was inoculated into the brain revealed mild spongiform change in two of these mice. Pathologic changes were observed unilaterally at only a single site in the corpus callosum (Fig. 5E). Pathologic changes were not observed in inoculated grey or white matter areas in the thalamus, pons, or colliculus. Because antigenic determinants for virus were destroyed when the CNS was prepared for histology, colocalization of infected cells in these two animals was not possible. In contrast to the immunohistochemistry data, this result suggests that some minimal level of viral infection in the CNS parenchyma occurred in P10 mice when exposed to virus alone. This finding supports the contention that cells in the CNS parenchyma are infectable beyond P10.

To evaluate the extent of astrocyte activation induced as a result of implantation with infected or uninfected microglia, implantation sites were evaluated immunohistochemically for increased GFAP expression. Although significant GFAP immunostaining was observable 5 days postimplantation at the site of transplants (Fig. 6A), staining was only marginally greater than in uninoculated controls (not shown). More significantly, no apparent glial scarring appeared to be associated with the implant (compared, for example, with Fig. 2A). Examination of GFAP staining at the time spongiform pathology was observable (21 days postimplantation) also indicated minimal astroglial activation at the sites of pathology both along the corpus callosum and in the thalamus (Fig. 6B and C). Low-level GFAP staining was also observed at the implant site in the thalami of control implanted animals despite the lack of spongiform change. This allowed for the identification of implant sites in the absence of the fluorescent cellular markers or spongiform change. Staining for microglial activation in implanted animals by Mac-1 failed to indicate any microglial activation under any inoculation regimen (not shown), again indicating that glial activation was limited in the implant model. The immunohistochemical and histopathological results observed for the implant experiments are summarized in Table 1.

A comparison of disease features observed in the wounding and implantation experiments, and after neonatal inoculation (Table 1), indicates potential common determinants in the induction of spongiform pathology. Note that the presence of CNS infection along with intense gliosis correlates with a lack of spongiosis, whereas parenchymal infection with an absent of mild glial response correlates with the expression of spongiform degeneration in both neonatally inoculated and microglia implant mice.

DISCUSSION

In this report, we have examined the developmental restriction to CNS infection which evolves as a function of advancing age and is observed in spite of high levels of peripheral virus replication (12, 13). The chronic exposure of endothelial cells to the circulating virus fails to result in their infection and the subsequent infection of the CNS parenchyma. However, when this endothelial barrier was bypassed by either injuring the CNS or implanting infected microglia, limited parenchymal infection was observed. This finding suggests that beyond P10, cells within the CNS parenchyma are still susceptible to virus infection, even though the entry of virus may be restricted. Whether the restriction at the blood-brain barrier is related to the mitotic capacity of vascular cells or the downregulation of virus receptor is not known. It is likely, though, that cessation of cell division for a variety of CNS cell types would be enough to restrict their infection (65).

The appearance of the developmental restriction has allowed us to generate focal models of virus infection and, in one instance, spongiform pathology. The first approach took advantage of the dynamics of wound repair in the CNS, where an acute stab injury results in the migration of inflammatory cells into the wound site, most notably cells of monocytic lineage, and activation and cell division of microglia and astrocytes (6, 16, 21, 25, 27, 52, 58). In the face of an ongoing peripheral infection, the glial cell division appeared to provide targets in the CNS parenchyma for virus infection. Parenchymal infection appeared to consist primarily of activated microglial cells, with infected monocytes appearing along the wound site. Despite the infection of CNS cells, there was a notable lack of spongiform lesions. In the second set of experiments, infected microglia were transplanted directly into the CNS of P10 mice. This resulted in both engraftment of the transplanted cells and the infection of endogenous parenchymal cells of a highly ramified nature. Infection was not seen in endothelial cells or in neurons which divide postnatally. The transplantation and

FIG. 5. Distribution of spongiform lesions parallels the location of $FrCas^E$ cells in transplanted animals. (A) Typical histopathology associated with the corpus callosum ipsilateral to the implant site. The contralateral corpus callosum (B) also shows spongiform change consistent with the distribution of virus-positive cells. (C) Thalamic pathology ipsilateral to the infected microglial implant. No pathology is observed on the contralateral side (D). Mild vacuolar pathology was occasionally observed in the corpus callosum of animals intracerebrally inoculated with $FrCas^E$ virus alone (E). Pathology was restricted to the corpus callosum at the site of injection. Pathology was not observed in the thalamus or colliculus/pons in any of the five animals examined. Implantation of infected microglia in the colliculus/pons resulted in unilateral pathology in grey matter areas. An example of the pathology in the posterior colliculus is shown in panel F. Areas of the pons showed patches of pathology (arrowheads, G) suggesting cellular migration of the implanted cells or specific neuronal susceptibility. The white-grey interface adjacent to the corticospinal tract in the pons was severely affected by the implanted infected microglial cells (H). This pathology was similar to that seen along the corpus callosum in that it appeared to be bilaterally symmetrical. Magnifications: (A to E) ×100; (F and G) ×50; (H) ×250.

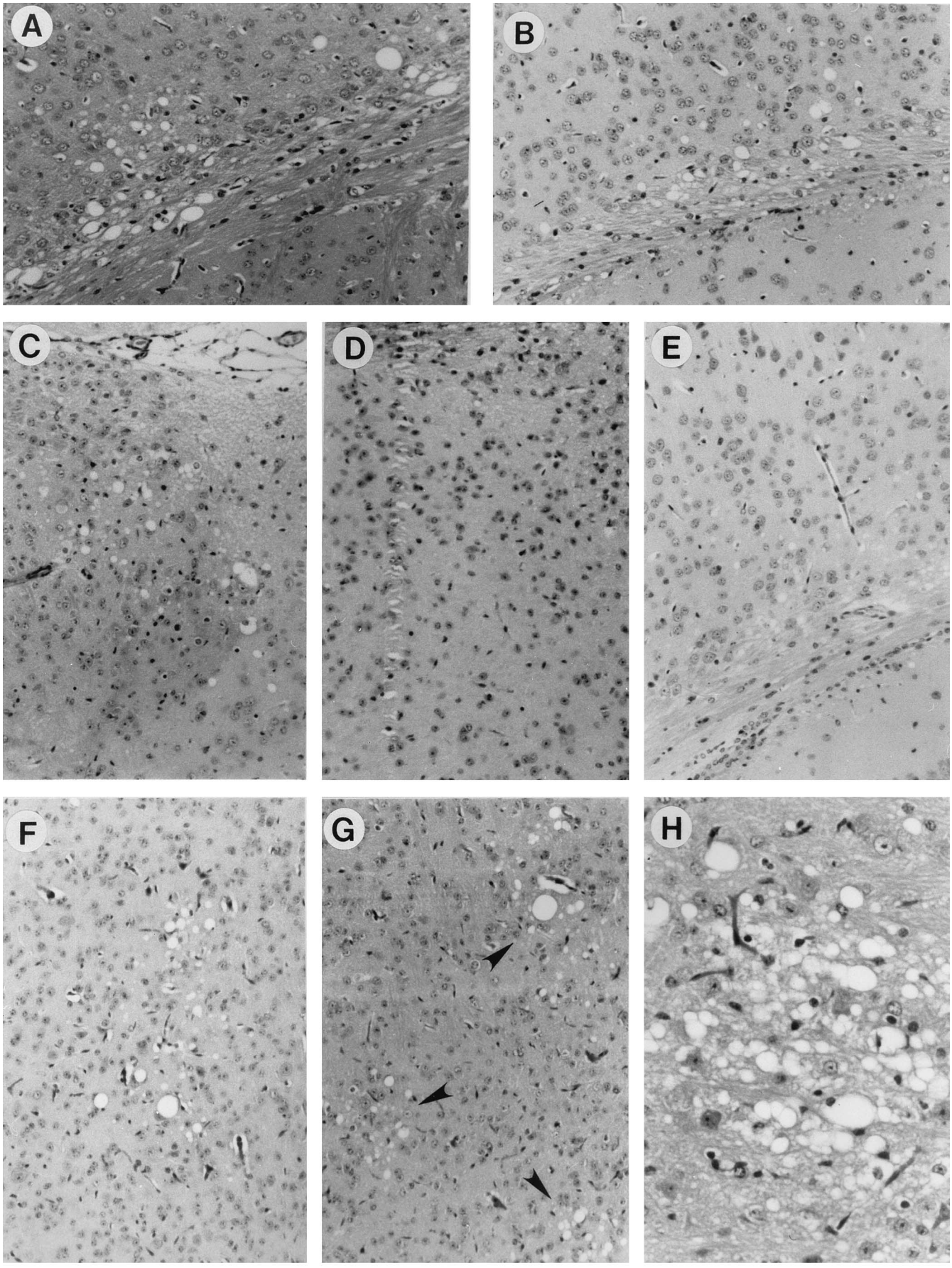
A
B
C
D
E
F
G
H

FIG. 6. Implant-associated astrogliosis is limited at the sites of spongiform pathology. (A) Astrocyte immunofluorescence staining (green) in a fresh-frozen section at the site where PKH-26-labeled FrCas^E-infected microglia (yellow-orange) were injected, 5 days postinoculation. Minimal glial activation is noted at this time. GFAP immunohistochemistry on paraffin sections (4 μm) at the time pathology was detectable (21 days postinoculation) also indicates limited astrocytic reaction (red staining) in the corpus callosum (B) and the thalamus (C). Magnifications: (A) ×200; (B) ×25; (C) ×200.

infection were unaccompanied by significant gliosis and gave rise to focal spongiform lesions within 21 days.

It has been reported that monocytic cells infected with human immunodeficiency virus secrete substances toxic to cultured neurons (29, 57). It has also been shown that activation of monocytic cells in the absence of infection results in the release of potentially toxic compounds, including reactive oxygen molecules (11, 23, 36, 42, 54), cytokines (24, 42), lipases (38), proteases (1), and specific neurotoxins (22, 26, 28). Thus, it might have been predicted that microglia/monocyte activation coincident with retrovirus infection should induce considerable pathology. It was surprising, then, that no spongiform lesions were observed in the wound model examined here. This observation is especially striking given the high level of neurovirulent retrovirus infection that was observed in areas of the CNS which are normally quite susceptible to retrovirus-induced degenerative changes (14, 46).

An attractive possibility as to why pathology was not observed in the wound paradigm is that the inflammatory response was able to prevent the normally toxic effects of the virus. This may be due to the expression of a variety of potentially neuroprotective molecules, including growth factors, cytokines, adhesion molecules, cytoskeletal proteins, receptors, and immune recognition molecules, which are released or upregulated in response to CNS injury (reviewed in references 16 and 22). For example, a recent report indicates that ciliary neurotrophic factor (CNTF) mRNA is dramatically upregulated in astrocytes in response to a mechanical lesion and is sustained for at least 20 days within the glial scar. Furthermore, significant CNTF neurotrophic activity is associated with soluble extracts of the lesioned tissue (34). This is particularly significant since motor neuron degeneration is the primary effect of neurovirulent murine retrovirus infection of the CNS. CNTF has been demonstrated to promote the survival of motor neurons both after axotomy (59) and in two murine mutant motor neuronopathies (50, 60). It would be of interest to determine whether CNTF alone can prevent the degenerative changes induced by FrCas^E.

The suggestion that glial activation may be neuroprotective might appear to be incongruous with findings from other models of retrovirus-induced neurodegeneration, wherein spongiform changes and glial activation are coincident (5, 8, 37, 51, 55). This observation, however, does not rule out the potential for glial activation to have a mitigating effect on degenerative processes. In the wound model, glial activation is present before, or at least coincident to, infection and occurs at levels that are more pronounced than that associated with spongiform change. Thus, glial activation may be able to act in a preventative manner to halt degeneration before it has been initiated. It is also possible that the expression of gliosis with spongiosis in part explains why the disease course is more protracted in these other models of retrovirus-induced neurodegeneration.

Alternative explanations as to why pathology may not have been observed in the wounding paradigm include the possibility that exposure of the CNS to virus at P17 fails to result in the infection of a critical subpopulation of cells. While vascular and monocytoid cells were observed to be infected in the wounding experiment, the infection of additional macroglia and neurons could not be discerned. Perhaps oligodendroglial cell infection, as observed in slower CasBrE disease models (8, 51, 53, 55), is necessary for observation of spongiform degeneration, although such infection was not observed in the rapid FrCas^E model. A more trivial explanation as to why pathology was not observed in the wound experiment is that susceptible sites for neurovirulent retrovirus interaction were acutely destroyed or downregulated with the wound itself.

The microglial transplant model presents an interesting contrast to the stab wound model, since only limited glial activation was observed and spongiform pathology was induced. The observation that the transplanted microglial cells failed to remain reactive to the Mac-1 and F4/80 antibodies and the lectin RCA-1, despite being identifiable with the fluorescent tracer DiI-AcLDL or PKH-26, is consistent with previous reports indicating that nonactivated microglial cells are not easily identifiable by specific cell surface and enzymatic markers in normal brains (19). This observation is also consistent with the normal development of microglia. Microglia enter the CNS perinatally as amoeboid cells, where they undergo cell division

and migrate to their ultimate sites of residence. In the process of taking up residence, they differentiate into highly ramified cells and downregulate many macrophage enzymatic and surface markers (19, 40, 43, 58). However, upon activation, the microglia revert to a more amoeboid morphology and increase the expression of these markers (18, 19, 21). The lack of microglial activation noted in the transplant model suggests that the inflammatory toxins described by Giulian et al. (26) are unlikely to be involved in the induction of spongiform pathology.

In the microglial transplant experiments wherein fluorescent tracers were used to mark the transplanted cells, the majority of infected cells observed did not contain the tracers. This finding indicates that the infected cells primarily represented endogenous CNS cells rather than transplanted cells which had lost the tracer. Although microglial cells infected with FrCas^E fail to release significant levels of infectious virions in vitro, they are highly capable of infecting permissive target cells as infectious centers (45). Presumably, transplantation of infected microglia results in complementation of the in vitro defect analogous to that seen in the infectious center assay (45). This idea is consistent with observations in two neonatal models of retrovirus-induced neurodegeneration caused by *ts*1 and FrCas^E, which indicated that microglial infection is productive (4, 5, 46).

The infection of CNS parenchymal cells by transplanted cells is of interest given that the endogenous parenchymal cells were relatively refractory to the challenge with free-virus inoculations. This finding suggests that the transient nature of a direct inoculation of free virus is not sufficient for the establishment of detectable CNS infection. This may be due to the limited half-life of the virus, its failure to be retained in the CNS parenchyma, or a limited expression of viral receptors in P10 brains. Whatever the specific mechanism, persistent exposure via cellular transplant appears to be capable of overcoming this parenchymal resistance and is sufficient for the induction of spongiform change.

Spongiform pathology coincident with cellular infection at the sites of transplantation and along white matter tracks in developmentally resistant animals indicates that the infected cells play a pivotal role in neuropathogenesis. So, what is the nature of the infected cells? In mice neonatally inoculated with neurovirulent murine retroviruses, many different cell types have been observed to be infected including endothelial cells, pericytes, microglia, oligodendroglia, astrocytes, and certain populations of neurons (4, 20, 30, 37, 46, 51, 55, 68). Which of these elements is involved in the pathogenesis of the disease has been a matter of speculation. The microglial transplant model presented herein directly addresses the potential involvement of vascular and neuronal infection. The failure to observe infection of endothelial cells and pericytes in mice transplanted with infected microglia suggests that they are not an absolute requirement for the induction of neuropathology. In similar fashion, infection of postnatally mitotic neurons in the cerebellum, dentate gyrus of the hippocampus, and cerebral cortex was also not observed in the microglial transplant model. Thus, downstream signal disruption by such neurons suggested previously (46) appears to be ruled out as the means for pathology induction.

If the infected cells are not neuronal or vascular, what are the other possible identities of these cells? Notably cells in subventricular germinal layer are known to give rise to macroglia postnatally. These glial progenitors, along with microglia, migrate along the corpus callosum on route to their final place of residence in white and grey matter regions. Furthermore, grey matter areas also contain macroglial progenitors which are known to divide throughout the life of the animal, presenting additional potential targets for infection. Nevertheless, immunohistochemical staining for astrocytes and oligodendroglia (macroglia) failed to show colocalization with viral antigen. However, macroglia are infectable in vitro with FrCas^E or *ts*1 Moloney murine leukemia virus, in which case they coexpress viral proteins and astrocyte (45, 61)- and oligodendrocyte (45)-specific markers. In addition, in vivo, CasBrE virus expression has been observed in cells bearing macroglia-specific markers (30, 51, 53). Thus, the results presented here suggests that if macroglial progenitors are infected, then expression of virus upon differentiation into identifiable astrocytes and oligodendroglia is somehow limited.

The morphology and location of the infected cells in the microglial transplant model were highly reminiscent of ramified microglia (58), which suggests a possible role for these cells in the development of spongiosis. However, without the ability to identify quiescent microglial cells in IRW mice, their identity as the infected cell type can only be inferred by exclusion of other cells. But since macroglial progenitors are also not readily identifiable, both microglia and macroglia must be considered as potentially mediating the observed local pathology in the transplant paradigm.

An alternative way of viewing the data from the transplant experiment would be to suggest that expression of virus or viral envelope protein by any cell type in close proximity to susceptible neurons is enough to elicit spongiform change. This could account for the findings from various laboratories implicating a variety of cell types. To determine this, engraftment of various infected cell types into mice in which the parenchymal cells are refractory to infection will be required. Alternatively, the generation of transgenic mice exhibiting cell-specific viral expression would also provide a means for identifying the specific cells responsible for inducing spongiform neurodegenerative disease.

In summary, we interpret the results presented here to indicate that (i) the developmental restriction to CNS infection developing by P10 can be bypassed by circumventing the blood-brain barrier through wounding or transplanting of infected cells, (ii) infection of the CNS in the presence of a CNS inflammatory response fails to result in spongiform pathology, (iii) exogenous FrCas^E-infected or uninfected microglial cells can engraft into the CNS of P10 mice (iv) engraftment of infected microglia can result in CNS parenchymal infection which colocalizes with the appearance of spongiform pathology, and (v) infection of endothelium and neurons which divide postnatally is not required to induce spongiform neuropathology.

ACKNOWLEDGMENTS

We thank A. Sharpe, W. Maury, B. Caughey, R. Bessen, and B. Chesebro for critical review of the manuscript. We also thank B. Evans and G. Hettrick for help with the figures.

REFERENCES

1. **Adams, D. O.** 1980. Effector mechanisms of cytologically activated macrophages. I. Secretion of neutral proteases and effect of protease inhibitors. J. Immunol. **124:**286–292.
2. **Austyn, J. M., and S. Gordon.** 1981. F4/80, a monoclonal antibody directed specifically against the mouse macrophage. Eur. J. Immunol. **11:**805–815.
3. **Barrett, C. P., E. J. Donati, and L. Guth.** 1984. Differences between adult and neonatal rats in their astroglial response to spinal injury. Exp. Neurol. **84:**374–385.
4. **Baszler, T. V., and J. F. Zachary.** 1990. Murine retroviral-induced spongiform neuronal degeneration parallels resident microglial cell infection: ultrastructural findings. Lab. Invest. **63:**612–623.
5. **Baszler, T. V., and J. F. Zachary.** 1991. Murine retroviral neurovirulence correlates with an enhanced ability of virus to infect selectively, replicate in,

and activate resident microglial cells. Am. J. Pathol. **138:**655–671. (Erratum, **138:**1058.)
6. **Bignami, A., and D. Dahl.** 1976. The astroglial response to stabbing. Immunofluorescent studies with antibodies to astrocyte-specific protein (GFA) in mammalian and submammalian vertebrates. Neuropathol. Appl. Neurobiol. **2:**99–110.
7. **Bignami, A., L. F. Eng, D. Dahl, and C. T. Uyeda.** 1972. Localization of glial fibrillary acidic protein in astrocytes by immunofluorescence. Brain Res. **43:**429–435.
8. **Brooks, B. R., J. R. Swarz, and R. T. Johnson.** 1980. Spongiform polioencephalomyelopathy caused by a murine retrovirus. Lab. Invest. **43:**480–486.
9. **Cobbold, S. P., A. Jayasuriya, A. Nash, T. D. Prospero, and H. Waldmann.** 1984. Therapy with monoclonal antibodies by elimination of T-cell subsets in vivo. Nature (London) **312:**548–551.
10. **Coffman, R. L., and I. L. Weissman.** 1981. B220: a B cell-specific member of the T200 glycoprotein family. Nature (London) **289:**681–683.
11. **Colton, C. A., and D. L. Gilbert.** 1987. Production of superoxide anion by a CNS macrophage, the microglia. FEBS Lett. **223:**284–288.
12. **Czub, M., S. Czub, F. McAtee, and J. Portis.** 1991. Age-dependent resistance to murine retrovirus-induced spongiform neurodegeneration results from central nervous system-specific restriction of virus replication. J. Virol. **65:** 2539–2544.
13. **Czub, M., F. J. McAtee, and J. L. Portis.** 1992. Murine retrovirus-induced spongiform encephalomyelopathy: host and viral factors which determine the length of the incubation period. J. Virol. **66:**3298–3305.
14. **Czub, S., W. P. Lynch, M. Czub, and J. L. Portis.** 1994. Kinetic analysis of the spongiform neurodegenerative disease induced by a highly virulent murine retrovirus. Lab. Invest. **70:**711–723.
15. **Dialynus, D. P., Z. S. Quan, K. A. Wall, A. Pierres, J. Quintans, M. R. Loken, M. Pierres, and F. W. Fitch.** 1983. Characterization of the murine T-cell surface molecule, designated L3T4, identified by monoclonal antibody GK 1.5: similarity of L3T4 to the human Leu-3/T4 molecule. J. Immunol. **131:** 2445–2451.
16. **Eddleston, M., and L. Mucke.** 1993. Molecular profile of reactive astrocytes—implications for their role in neurologic disease. Neuroscience **54:**15–36.
17. **Evans, L. H., R. P. Morrison, F. G. Malik, J. Portis, and W. J. Britt.** 1990. A neutralizable epitope common to the envelope glycoproteins of ecotropic, polytropic, xenotropic, and amphotropic murine leukemia viruses. J. Virol. **64:**6176–6183.
18. **Finsen, B. R., M. B. Jorgensen, N. H. Diemer, and J. Zimmer.** 1993. Microglial MHC antigen expression after ischemic and kainic acid lesions of the adult rat hippocampus. Glia **7:**41–49.
19. **Flaris, N. A., T. L. Densmore, M. C. Molleston, and W. F. Hickey.** 1993. Characterization of microglia and macrophages in the central nervous system of rats: definition of the differential expression of molecules using standard and novel monoclonal antibodies in normal CNS and in four models of parenchymal reaction. Glia **7:**34–40.
20. **Gardner, M. B., B. E. Henderson, J. E. Officer, R. W. Rongey, J. C. Parker, C. Oliver, J. D. Estes, and R. J. Huebner.** 1973. A spontaneous lower motor neuron disease apparently caused by indigenous type-C RNA virus in wild mice. J. Natl. Cancer Inst. **51:**1243–1254.
21. **Giulian, D.** 1987. Ameboid microglia as effectors of inflammation in the central nervous system. J. Neurosci. Res. **18:**155–171.
22. **Giulian, D.** 1993. Reactive glia as rivals in regulating neuronal survival. Glia **7:**102–110.
23. **Giulian, D., and T. J. Baker.** 1986. Characterization of ameboid microglia isolated from developing mammalian brain. J. Neurosci. **6:**2163–2178.
24. **Giulian, D., T. J. Baker, L. C. Shih, and L. B. Lachman.** 1986. Interleukin 1 of the central nervous system is produced by ameboid microglia. J. Exp. Med. **164:**594–604.
25. **Giulian, D., J. Chen, J. E. Ingeman, J. K. George, and M. Noponen.** 1989. The role of mononuclear phagocytes in wound healing after traumatic injury to adult mammalian brain. J. Neurosci. **9:**4416–4429.
26. **Giulian, D., M. Corpuz, S. Chapman, M. Mansouri, and C. Robertson.** 1993. Reactive mononuclear phagocytes release neurotoxins after ischemic and traumatic injury to the central nervous system. J. Neurosci. Res. **36:**681–693.
27. **Giulian, D., B. Johnson, J. F. Krebs, J. K. George, and M. Tapscott.** 1991. Microglial mitogens are produced in the developing and injured mammalian brain. J. Cell Biol. **112:**323–333.
28. **Giulian, D., K. Vaca, and M. Corpuz.** 1993. Brain glia release factors with opposing actions upon neuronal survival. J. Neurosci. **13:**29–37.
29. **Giulian, D., K. Vaca, and C. A. Noonan.** 1990. Secretion of neurotoxins by mononuclear phagocytes infected with HIV-1. Science **250:**1593–1596.
30. **Gravel, C., D. G. Kay, and P. Jolicoeur.** 1993. Identification of the infected target cell type in spongiform myeloencephalopathy induced by the neurotropic Cas-Br-E murine leukemia virus. J. Virol. **67:**6648–6658.
31. **Hestdal, K., F. W. Ruscetti, J. N. Ihle, S. E. Jacobsen, C. M. Dubois, W. C. Kopp, D. L. Longo, and J. R. Keller.** 1991. Characterization and regulation of RB6-8C5 antigen expression on murine bone marrow cells. J. Immunol. **147:**22–28.
32. **Hogan, B., F. Constantini, and E. Lacy.** 1986. Manipulating the mouse embryo, p. 186–187. Cold Spring Harbor Laboratory, Cold Spring Harbor, N.Y.
33. **Horan, P. K., M. J. Melnicoff, B. D. Jensen, and S. E. Slezak.** 1990. Fluorescent cell labeling for in vivo and in vitro cell tracking. Methods Cell Biol. **33:**469–490.
34. **Ip, N. Y., S. J. Wiegand, J. Morse, and J. S. Rudge.** 1993. Injury-induced regulation of ciliary neurotrophic factor mRNA in the adult rat brain. Eur. J. Neurosci. **5:**25–33.
35. **Jeffrey, M., and G. A. H. Wells.** 1987. Cell markers in the central nervous system. Vet. Bull. **57:**247–266.
36. **Johnston, R. B., C. A. Godzik, and Z. A. Cohn.** 1978. Increased superoxide anion production by immunologically activated and chemically elicited macrophages. J. Exp. Med. **148:**115–127.
37. **Kay, D. G., C. Gravel, Y. Robitaille, and P. Jolicoeur.** 1991. Retrovirus-induced spongiform myeloencephalopathy in mice: regional distribution of infected target cells and neuronal loss occurring in the absence of viral expression in neurons. Proc. Natl. Acad. Sci. USA **88:**1281–1285.
38. **Khoo, J. C., E. M. Mahoney, and J. L. Witztum.** 1981. Secretion of lipoprotein lipase by macrophages in culture. J. Biol. Chem. **256:**7105–7108.
39. **Ledbetter, J. A., and L. A. Herzenberg.** 1979. Xenogeneic monoclonal antibodies to mouse lymphoid differentiation antigens. Immunol. Rev. **47:**63–90.
40. **Leong, S.-K., and E.-A. Ling.** 1992. Ameboid and ramified microglia: their interrelationship and response to brain injury. Glia **6:**39–47.
41. **Levinson, S. W., and K. D. McCarthy.** 1991. Astroglia in culture, p. 309–336. *In* G. Banker and K. Goslin (ed.), Culturing nerve cells. The MIT Press, Cambridge, Mass.
42. **Liew, F. Y., and F. E. Cox.** 1991. Nonspecific defense mechanism: the role of nitric oxide. Immunol. Today **12:**A17–A21.
43. **Ling, E.-A., and W.-C. Wong.** 1993. The origin and nature of ramified and amoeboid microglia: a historical review and current concepts. Glia **7:**9–18.
44. **Lynch, W. P.** Unpublished observations.
45. **Lynch, W. P., W. J. Brown, G. J. Spangrude, and J. L. Portis.** 1994. Microglia infection by a neurovirulent murine retrovirus results in defective processing of envelope protein and intracellular budding of virus particles. J. Virol. **68:**3401–3409.
46. **Lynch, W. P., S. Czub, F. J. McAtee, S. F. Hayes, and J. L. Portis.** 1991. Murine retrovirus-induced spongiform encephalopathy: productive infection of microglia and cerebellar neurons in accelerated CNS disease. Neuron **7:**365–379.
47. **Lynch, W. P., and J. L. Portis.** 1993. Murine retrovirus-induced spongiform encephalopathy: disease expression is dependent on postnatal development of the central nervous system. J. Virol. **67:**2601–2610.
48. **Matsumoto, Y., K. Watabe, and F. Ikuta.** 1985. Immunohistochemical study on neuroglia identified by the monoclonal antibody against a macrophage differentiation antigen (Mac-1). J. Neuroimmunol. **9:**379–389.
49. **McAtee, F. J., and J. L. Portis.** 1985. Monoclonal antibodies specific for wild mouse neurotropic retrovirus: detection of comparable levels of virus replication in mouse strains susceptible and resistent to paralytic disease. J. Virol. **56:**1010–1022.
50. **Mitsumoto, H., K. Ikeda, B. Klinkosz, J. M. Cedarbaum, V. Wong, and R. M. Lindsay.** 1994. Arrest of motor neuron disease in *wobbler* mice cotreated with CNTF and BDNF. Science **265:**1107–1110.
51. **Morey, M. K., and C. A. Wiley.** 1990. Immunohistochemical localization of the neurotropic ecotropic murine leukemia virus in moribund mice. Virology **178:**104–112.
52. **Mucke, L., M. B. A. Oldstone, J. C. Morris, and M. I. Nerenberg.** 1991. Rapid activation of astrocyte-specific expression of GFAP-lacZ transgene by focal injury. New Biol. **3:**465–474.
53. **Nagra, R. M., P. G. Burrola, and C. A. Wiley.** 1992. Development of spongiform encephalopathy in retroviral infected mice. Lab. Invest. **66:**292–302.
54. **Nathan, C. F., and R. K. Root.** 1977. Hydrogen peroxide release from mouse peritoneal macrophages. J. Exp. Med. **146:**1648–1662.
55. **Oldstone, M. B. A., P. W. Lampert, S. Lee, and F. J. Dixon.** 1977. Pathogenesis of the slow disease of the central nervous system associated with WM 1504 E virus. Am. J. Pathol. **88:**193–212.
56. **Portis, J. L., S. Czub, C. F. Garon, and F. J. McAtee.** 1990. Neurodegenerative disease induced by the wild mouse ecotropic retrovirus is markedly accelerated by long terminal repeat and *gag-pol* sequences from nondefective Friend murine leukemia virus. J. Virol. **64:**1648–1656.
57. **Pulliam, L., B. G. Herndier, N. M. Tang, and M. S. McGrath.** 1991. Human immunodeficiency virus-infected macrophages produce soluble factors that cause histological and neurochemical alterations in cultured human brains. J. Clin. Invest. **87:**503–512.
58. **Rio-Hortega, P. D.** 1932. Microglia, p. 481–534. *In* W. Penfield (ed.), Cytology & cellular pathology of the nervous system. Hafner Publishing Company, New York.
59. **Sendtner, M., G. W. Kreutzberg, and H. Thoenen.** 1990. Ciliary neurotrophic factor prevents the degeneration of motor neurons after axotomy. Nature (London) **345:**440–441.
60. **Sendtner, M., H. Schmalbruch, K. A. Stockli, P. Carroll, G. W. Kreutzberg, and H. Thoenen.** 1992. Ciliary neurotrophic factor prevents degeneration of motor neurons in mouse mutant progressive motor neuronopathy. Nature (London) **358:**502–504.

61. **Shikova, E., Y. C. Lin, K. Saha, B. R. Brooks, and P. K. Wong.** 1993. Correlation of specific virus-astrocyte interactions and cytopathic effects induced by *ts*1, a neurovirulent mutant of Moloney murine leukemia virus. J. Virol. **67:**1137–1147.
62. **Springer, T., G. Galfre, D. S. Secher, and C. Milstein.** 1979. Mac-1: a macrophage differentiation antigen identified by monoclonal antibody. Eur. J. Immunol. **9:**301–306.
63. **Sternberger, N. H.** 1984. Patterns of oligodendrocyte function seen by immunohistochemistry, p. 125–173. *In* W. T. Norton (ed.), Oligodendroglia. Plenum Press, New York.
64. **Tomonari, K.** 1988. A rat antibody against a structure functionally related to the mouse T-cell receptor/T3 complex. Immunogenetics **28:**455–458.
65. **Varmus, H., and R. Swandstrom.** 1982. Replication of retroviruses, p. 467–469. *In* R. Weiss, N. Teich, H. Varmus, and J. Coffin (ed.), RNA tumor viruses: molecular biology of tumor viruses. Cold Spring Harbor Laboratory, Cold Spring Harbor, N.Y.
66. **Wong, P. K. Y., and P. H. Yuen.** 1992. Molecular basis of neurologic disorders induced by a mutant ts1, of Moloney murine leukemia virus, p. 161–197. *In* R. Roos (ed.), Molecular Neurovirology: pathogenesis of viral CNS infections. Humana Press, Totowa, N.J.
67. **Yagita, H., T. Nakamura, H. Karasuyama, and K. Okumura.** 1989. Monoclonal antibodies specific for murine CD2 reveal its presence on B as well as T cells. Proc. Natl. Acad. Sci. USA **86:**645–649.
68. **Zachary, J. F., C. J. Knupp, and P. K. Y. Wong.** 1986. Non-inflammatory spongiform polioencephalomyelopathy caused by a neurotropic temperature-sensitive mutant of Moloney murine leukemia virus TB. Am. J. Pathol. **124:**457–468.

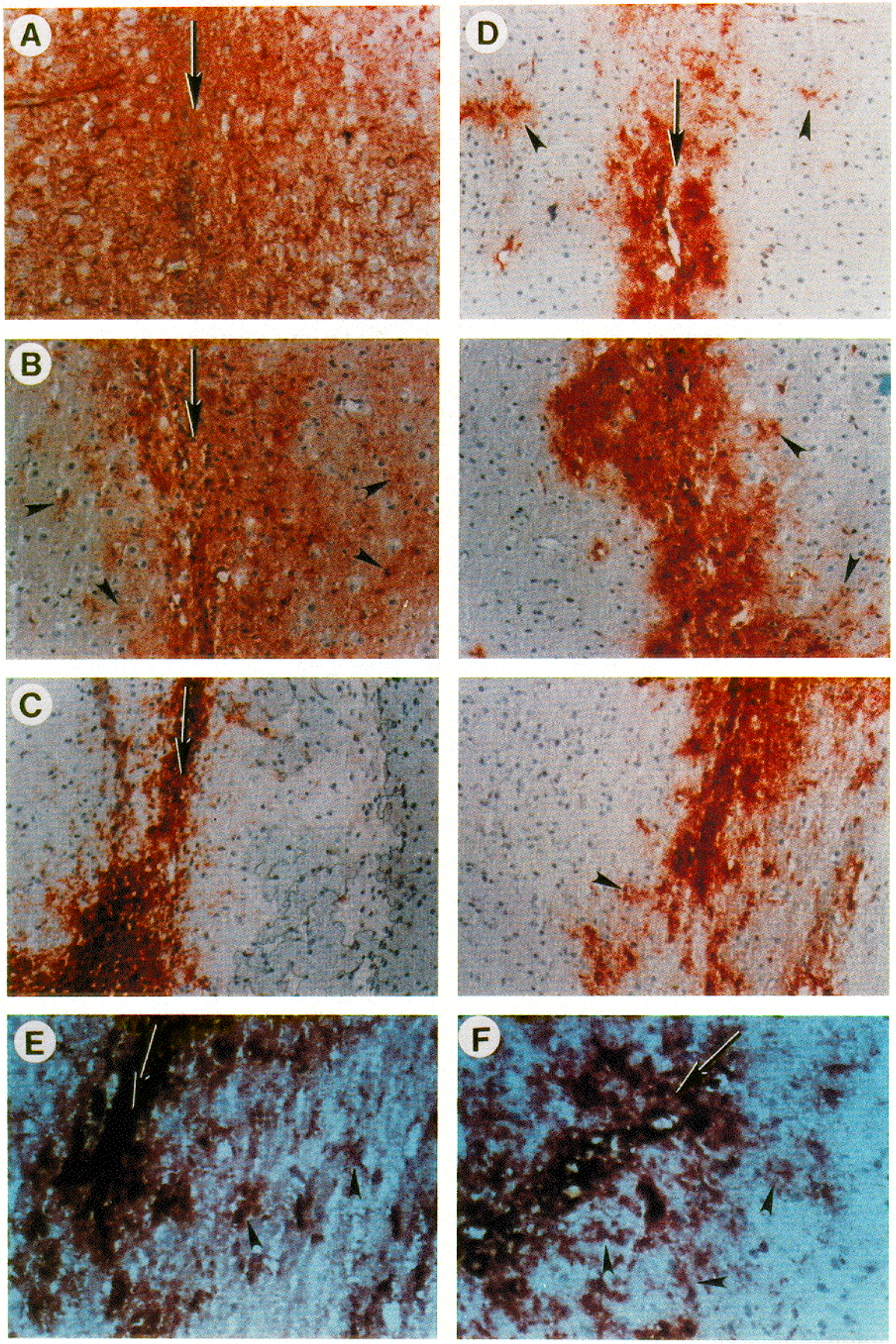
A
D
B
C
E
F

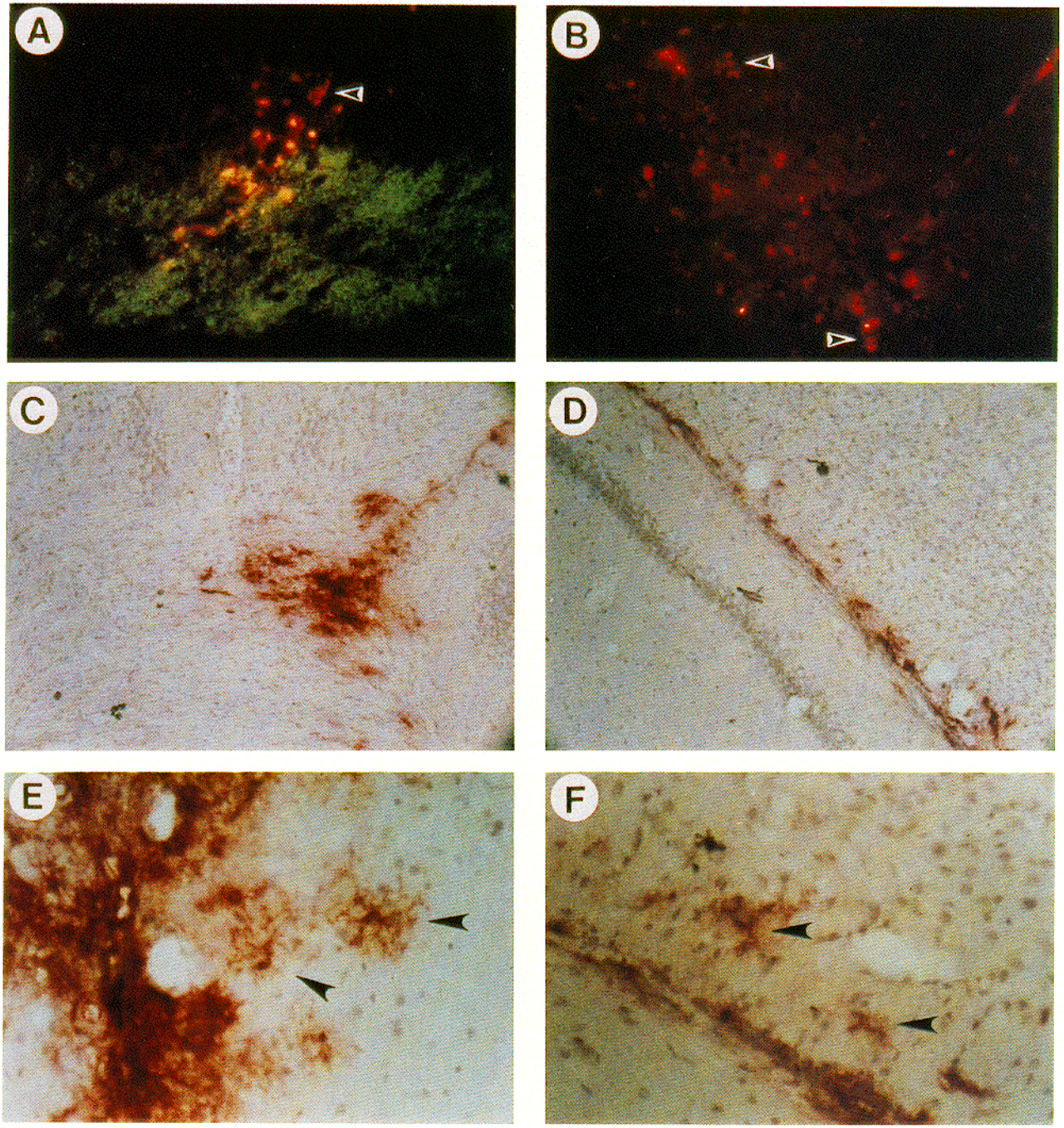
A
B
C
D
E
F

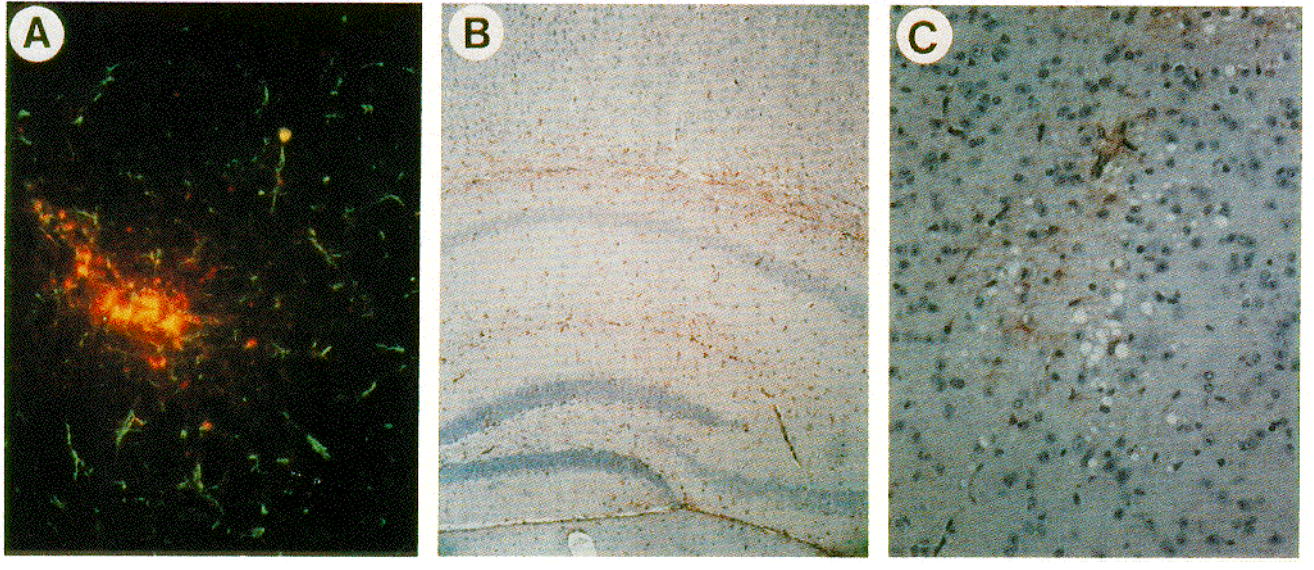
A
B
C